Experimental and Modeling of Tomato Slices Sorption Isotherms and Thin Layer Drying Kinetics for a Solar Drying Plant Design

Jmai, Sana**+; Ben Slimane, Nihel; Guiza, Sami; Messaoudi, Saif Eddine; Mohamed, Bagane

Applied Thermodynamic Laboratory, National School of Engineers of Gabes Tunisia, Medina Street 6029, University of Gabes, TUNISIA

ABSTRACT: *In the present work, the sorption isotherms of Tomato Slices (TS) are obtained by the gravimetric method at different temperatures (50, 60, and 70 °C). After fitting the desorption curves, the Guggenheim-Anderson-de Boer (GAB) model is chosen as the most appropriate model for the experimental data of tomato slice desorption isotherm. The isosteric heat of desorption is then determined by the Clausius-Clapeyron equation. Modeling of the convective drying kinetics is performed by experimental study of the effects of aerothermal conditions, such as temperature and hot air velocity. The drying characteristic curves are then fitted using MATLABR 2013 nonlinear regression- functions. The parabolic model was found to be the most appropriate model for the experimental results of kinetic drying of tomato slices, with the highest R^2 correlation coefficient average value (0.9983) and the lowest RMSE average value (0.0119). The effective moisture diffusivity and the activation energy are tested by the second Fick's law. The values of effective moisture diffusivity ranged from 2.028 10^{-7} to 5.071 10^{-7} m^2/s. The activation energy was calculated to be 42.140 kJ/mol.*

KEYWORDS: *Tomato; Gravimetric method; Moisture transfer parameters; Effective moisture diffusivity, Kinetics and thermodynamics modeling; Solar dryer design.*

INTRODUCTION

Energy prices in the world have already increased significantly for several months. For the year 2022, an increase of more than 30% is estimated according to many experts. As a result, more states could impose demand-limiting measures for oil and gas. It is also possible that consumers, including industrialists and citizens, must reduce their consumption, especially in terms of heating.

In short, the impact of the war in Ukraine on the energy market is already being felt. Since the start of this war, fuel and gas prices have risen. Several states find themselves in a delicate situation. In addition, the health crisis caused by the Covid-19 pandemic has already damaged the energy sector.

To no longer suffer the impact of rising energy prices on the wholesale market, the ideal is to promote the development of renewable energies. The goal is to achieve

**To whom correspondence should be addressed.*
+ E-mail: sanajmai1@gmail.com & sana.jmai@enig.rnu.tn
1021-9986/2023/8/2687-2703 17/$/6.07

energy independence.

If the effect of this crisis is huge on developed countries what about its impact on third-world or developing countries if they do not have oil and gas.

So, thinking seriously about renewable energy is the only way out for these countries. Accordingly, the availability of solar energy and the operational marketing and economic reasons offer a good opportunity for using solar drying all over the world. A great number of successful practical applications have already been reported. Many countries must orient their savings, energy investments and the strategy of research programs in the field of energy towards solar energy. This is the case of Tunisia (not an oil and gas producing country), which is suffering enormously from soaring energy prices due to economic and social problems, which affect the political stability of the country.

In Tunisia, solar energy is a permanent, inexhaustible and free source. The sudden increase in the price of oil led the state to take an interest in renewable energy sources, first and foremost solar energy. The main characteristics of solar energy that aroused interest in it at the time were its free nature, its availability, and the absence of the risk of exhaustion known by the sources of energy 'fossil fuels. Many investigations demonstrated the benefits of solar drying under Tunisian climate, and social and economic conditions.

We quickly realized that solar energy, contrary to popular belief, is not entirely free: Its use requires an initial investment that is often heavier than for conventional energy sources and a number of installations. Solar systems are now shut down because they have not provided a budget for the maintenance of the equipment.

The uptake of radiation cannot be considered random. It is easy to calculate with correct precision the ideal solar power that can be available on a site at a given time if the sky is clear, but the real power received on a collector can vary between 10 to 110 % of this ideal power depending on the instantaneous local content of the atmosphere in water and various dust.

We have chosen, under the prevailing climatic conditions in the South of Tunisia, a locally produced product as a model: Tomatoes. The design program the of drying system could be used to calculate drying parameters for similar products under different climatic conditions.

Solar drying represents a simple and low-cost method to preserve agricultural products for the off-season. Tomatoes are rich in a number of functional health constituents, such as the red carotenoid lycopene and various other flavonoids, ascorbic acid, and phenolic acids (especially chlorogenic acids) in addition to basic nutritional compounds [1, 2]. The elevated antioxidant levels found in tomatoes and tomato foods assist in impeding the harmful oxidative harm to the body [3]. Lycopene is a carotenoid compound found naturally in tomatoes, tomato-processed materials, and various fruits. The dietary consumption of lycopene-containing nutrients results in a decreased risk of chronic diseases, involving cancer and cardiovascular diseases. *Cheng et al*.(2017) [4] have reported that the plasma levels of lycopene and other carotenoids can be enhanced by the ingestion of realistically small amounts of tomato juice. Lycopene seems to be equally bioavailable from tomatoes and other nutrient supplements.

The product can be modified to satisfy various consumer demands. Generally, processed products leave lower in nutritive capacity than their corresponding products, mostly due to the losses in nutritional constituents, such as vitamins, during treatment [5,6]. Nevertheless, Akshay *Sonawane et al*. [7] have proposed that lycopene levels were greater in thermally treated tomatoes than in non-treated tomatoes. *Ahmed Djebli et al*. [8] have suggested that greater antioxidant activities are obtained by heat processing such as cooking, steaming, microwaving and frying of tomatoes.

Drying is one of the most ancient and effective ways to preserve food from spoilage. This method can affect the structural and physical changes that may include migration of dissolvable solids, shrinkage and hardening of the case, reduction of volatiles and flavors, and reduced water absorption upon rehydration. To reduce these effects, drying methods such as freeze-drying, low-temperature air drying and vacuum drying are used [9,10]. When dried, numerous foods can be preserved for many years without refrigeration, provides a proper packaging [11]. Tomatoes are usually dehydrated at elevated temperature levels in the presence of oxygen, and dehydrated tomato products (tomato halves, slices, wedges and powders) are the most sensitive to oxidative destruction [12,13]. Although a number of technologies can be used for biomass drying, depending on the heat transfer mode used for drying (microwave [14,15], conduction [16],

convection [17] , radiation [18] or combined mode), purely convective dryers using hot air (HAD) or flue gas currently account for more than 80 % of the adopted industrial biomass dryers [19,14]. The hot air dryer is a popular and simple way to dry food materials [18]. Many scientists have studied hot air drying on specification of fruits and vegetables, such as banana [21], almond [22] , onion [23], Whole Lemons [24], and grape seeds [25].

Many scientific research papers have been published in the literature to increase the solar air collector's thermal performance *Sajawal* [26] has increased the thermal performance of the double-pass solar air collector with phase change materials (PCM) found in finned metal tubes. *Aboghrara et al*.[27] have designed circular jets to enhance the solar collector airflow inside the air duct. They have examined the impact of jet collisions on corrugated absorber plate using circular jets. They stated that with the improved airflow they achieved, heat transfers in the corrugated absorber plate increased and the air mass flow rate increased the thermal performance in the solar air collector. The thermal performance of the solar air collectors was increased by *Mzad et al*. [28] using aluminum thermal storage on days with weak sunlight aluminum thermal storage on days. *Nidhal et al*. [29] has studied the effects of ribs on thermal performance of curved absorber 1 tube used in cylindrical solar collectors. The efficiency of aqueous solar cells: a photo electrochemical estimation on the effectiveness of $TiCl_4$ treatment was studied by *Federico et al*. [30]. *Simone et al*. [31] has studied the Finely tuning electrolytes and photo anodes in aqueous solar cells by experimental design. When the Boosting electric double layer capacitance in laser-induced Graphene-based super capacitors was studied by *Marco et al*. [31].

The present study aims the designing of a solar tomato drying plant. Before this step, some specific information must be known about: (i) Drying time and energy consumption for the product under varying weather conditions, (ii) Evaluation of the product quality and (ii) Economic evaluation of the drying system.

Main factors affecting solar food dryers are: i) Relative humidity and ii) Solar radiation. Drying time is also affected by type of food and its water content, and thickness of slices.

An experimental study of desorption isotherms of wet tomato slices was carried out by the static gravimetric method based on saturated salt solutions. More precisely, the effect of target solids temperature (at three levels, i.e. 50, 60 and 70 °C) on drying was studied in batch mode. Subsequently, an experimental and theoretical study on tomato slices drying was investigated in order to study the effect of temperature and drying air velocity on the kinetic behavior during the drying process. The drying operation was performed in a hot air dryer worked in closed cycle and was equipped with a programmable controlling system for drying air parameters. The diffusivity coefficient and the activation energy were calculated from the analytical solution of the Fick equation.

The experimental protocol consists of:
1-Study of the thermodynamics and drying kinetics of the model product: (i) Determination of desorption isotherms, (ii) Calculation of the heat of desorption, (iii) Study of the effect of temperature and the speed of air flow on drying speed, and (iv) Modelling of thermodynamics and kinetics data. 2-Use of the previous collected data in the simulation of the solar process and sizing the equipment of the installation.

Many papers have focused on natural convection solar dryers, which are fully described, and many researchers have studied agricultural products and their characteristics while drying.

In this work, a new simple solar drying system is designed with the aim of drying 100 kg of locally produced tomato slices under the prevailing climatic conditions.

EXPERIMENTAL SECTION

Description of the installation

The dryer presented in Fig.1 is used to dry food products (Tomato). It is an indirect drying that uses ambient air heated to a determined temperature. This system works by forced convection and by partial solar heating. The electric auxiliary heating uses an electric resistance (thermal heat exchanger) fed by the electric network. An electrical energy supplement is necessary to compensate for the inability of the solar collector to maintain the temperature in the desired range during the periods of low light or night. Hot air arrives at the entrance of the drying chamber and crosses the racks, and at the outlet of the cabinet there is a fan that sucks the drying air through the overlapping racks and delivers it to the outside. This installation consists of the following units:

***Table 1: Water activities of saturated saline solutions* [35]**

Solution	Activities		
	50°C	60°C	70°C
KOH	5.7	5.5	5.3
K_2CO_3	45.6	45	-----
NaBr	50.9	49.7	49.7
KI	64.49	63.11	61.93
NaCL	74.4	74.5	75.1
KCL	81.2	80.3	79.5
$BaCl_2.2H_2O$	88.23	87.28	-----
K_2SO_4	95.8	95.7	-----

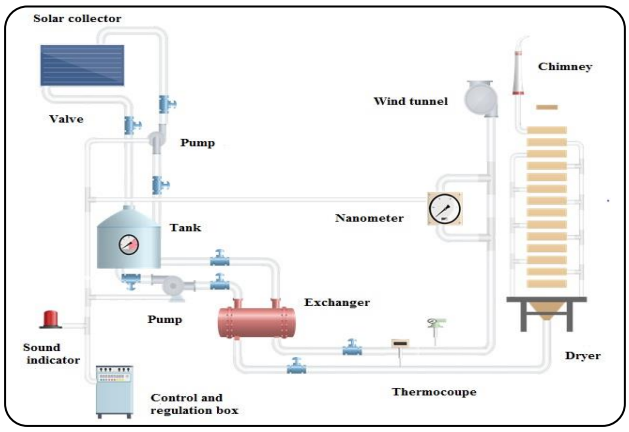

Fig.1: Solar tomato drying plant

-A drying chamber consisting of 10 superimposed trays on which the product to be dried is placed. The height of the drying chamber is 1.2 m, its length is 3 m and its width is 1.7 m. The external walls are made of Brik insulated with polystyrene.
-A solar collector, also called solar water heater, is a device for capturing solar radiation to provide the hot water.
-An exchanger that will exchange a quantity of heat from a hot fluid (water) to a cold fluid (air) to obtain an air flow at a designated temperature.
-The connecting pipes between the equipment.
-A regulator for measuring different temperatures and switching on or off a circulation pump.
-The hot water storage tank.
-Some essential parts that constitute a solar installation: an electric booster, an exchanger, a solar thermal probe, an expansion tank and a hydraulic set.

Desorption isotherms determination

Tomatoes variety (JAWARA F1) of uniform size and colour were purchased from the local market, Tunisia and stored in a refrigerator at 4 °C until use. The equilibrium moisture contents of the tomato samples were determined at 50, 60 and 70 °C by the static gravimetric method. The samples were put on a sample holder into hermetic jars, where eight saturated salt solutions KOH, K_2CO_3, NaBr, KI, NaCl, KCL, $BaCl_2.2H_2O$ and K_2SO_4 were used.

Water activity, aw, indicates the presence of free water in a product for the development of chemical reactions, spore and microorganism's germination [32]. It plays an essential role in the product stability resulting from vegetables due to the direct implication of the water in most chemical and biochemical reactions [33]. The water activity lowering of foods is one of the most common and oldest types of food conservation [34].

Table 1 shows that these saturated solutions have a water activity range from 0.053 to 0.958.

The test samples (0.5 ± 0.01 g) were enclosed in hermetically sealed chambers containing saturated salt solution, maintained at a constant temperature in an oven.

The weight variation had been several times registered, using a ± 0.001 g precision balance, at different time periods extending to several days. The hygroscopic equilibrium is supposed to be reached when the sample weight is the same in two successive measurements. Once the wet weights are determined, the samples are placed in an oven at 105 °C for 24 h to establish their dry weights [36].

The mass difference between the sample before and after drying in the oven was measured to determine the tomatoes water level at equilibrium X_{eq}:

$$X_{eq} = \frac{M_h - M_s}{M_s} \quad (1)$$

where M_h = the mass of the samples before drying;
M_s = the mass of the samples after drying;
X_{eq} = the water content of the samples at equilibrium

The analysis of the experimental data obtained for the equilibrium moisture content and water activity at different temperatures was performed using the various mathematical models presented in Table 2. The regression was carried out using the MATLAB R2013a computer program.

The adjustment between the established experimentally points and the model is judged by the correlation coefficient (R^2), the Root Means Square Error (RMSE) and the chi-square test (SSE). The model that has a relatively high R^2 and relatively low SSE and RMSE is the best model that suits the isotherm curves.

Table 2: Mathematical models tested to fit desorption isotherm

Model	Model equation		Reference
Smith	$Xeq = A - B.\ln(1 - aw)$	(2)	[37]
Iglesias and Chirife	$Xeq = A + B.\frac{aw}{1-aw}$	(3)	[38]
Caurie	$Xeq = e^{(A+B.aw)}$	(4)	[39]
White and Eiring	$Xeq = \frac{1}{A+B.aw}$	(5)	[39]
Peleg	$Xeq = A.aw^B + C.aw^D$	(6)	[40]
Guggenhein, Anderson, Boer	$Xeq = \frac{A.C.B.aw}{(1-B.aw)(1-B.aw+A.B.aw)}$	(7)	[41]
Oswin	$Xeq = A.(\frac{aw}{1-aw})^B$	(8)	[42]
Adam	$Xeq = A + B.aw + C.aw^2 + D.aw^3$	(9)	[43]
Halsey	$Xeq = (-\frac{A}{\ln(aw)})^{1/B}$	(10)	[44]
Langmuir	$Xeq = A.\frac{B.aw}{1+C.aw}$	(11)	[45]
Henderson	$Xeq = (-\frac{\ln(1-aw)}{A})^{1/B}$	(12)	[46]
Chung-Pfost	$Xeq = -\frac{1}{A}.\ln(T.R.\frac{\ln(aw)}{-B})$	(13)	[47]

$$R^2 = \sqrt{1 - \frac{\sum_{j=1}^{N}(X_{jcal} - X_{jexp})^2}{\sum_{j=1}^{N}(X_m - X_{jexp})^2}} \quad (14)$$

$$X_m = \frac{\sum_{j=1}^{N} X_{jexp}}{N} \quad (15)$$

$$SSE = \frac{100}{N} + \sum_{j=1}^{N} \left| \frac{X_{jcal} - X_{jexp}}{X_{jexp}} \right| \quad (16)$$

$$RMSE = \sqrt{\sum_{j=1}^{N} \frac{(X_{jcal} - X_{jexp})^2}{N - n_p}} \quad (17)$$

where:

R^2: The correlation coefficient;

X_{jcal}: The calculated values of the water content at equilibrium (kg water / kg db);

X_{exp}: The experimental values of the water content at equilibrium (kg water / kg db);

X_m: The value of the arithmetic mean of the experimental values of the water content at equilibrium (kg water / kg db)

N: The number of experimental points;

n_p: The number of model constants.

Isosteric heat

The differential enthalpy or the isosteric heat of sorption (ΔHd) is used to describe the phase of the emerging water in the solid. The net isosteric heat of sorption (Δhd) (Equation (18)) is the quantity of the energy above the heat of water vaporization (ΔHvap) (Equation (19)) related to the sorption operation. This property was determined relying on the experimental results by the Clausius-Clapeyron equation, which has been used by many authors. *Sana et al* have used this formula to establish the isosteric heat of di-calcium phosphate [48], *Abdenouri et al*. [49] have used it to establish the isosteric heat of milk powder and *Tsami et al*. [50] to establish the isosteric heat of the fruit.

$$\left(\frac{d(\ln(aw))}{d\left(\frac{1}{T}\right)}\right)_{Xeq} = \frac{-\Delta h_d}{R} \quad (18)$$

and

$$\Delta h_d = \Delta H_d - \Delta H_{vap} \quad (19)$$

The sorption isotherms at different temperatures needed to be studied to establish a logarithmic curve for the water activity variation with the inversed temperature, at a constant water content.

Obtaining the analytical expression for the heat of sorption Δhd is available from Equation (19).

The experimental points of the sorption isotherms were plotted as (ln(aw)) versus the equilibrium water content (Xeq). We obtained Δhd from the slope of the line (-ln (aw)) versus (1/T).

DRYING KINETICS STUDY

Experimental procedure

To guarantee a dried product with good quality, experiments were carried out in the temperature range of 50 to 70 °C, an air velocity range from 0.6 m/s to 1.4 m/s and fixed relative humidity at 30 %. Convective driers

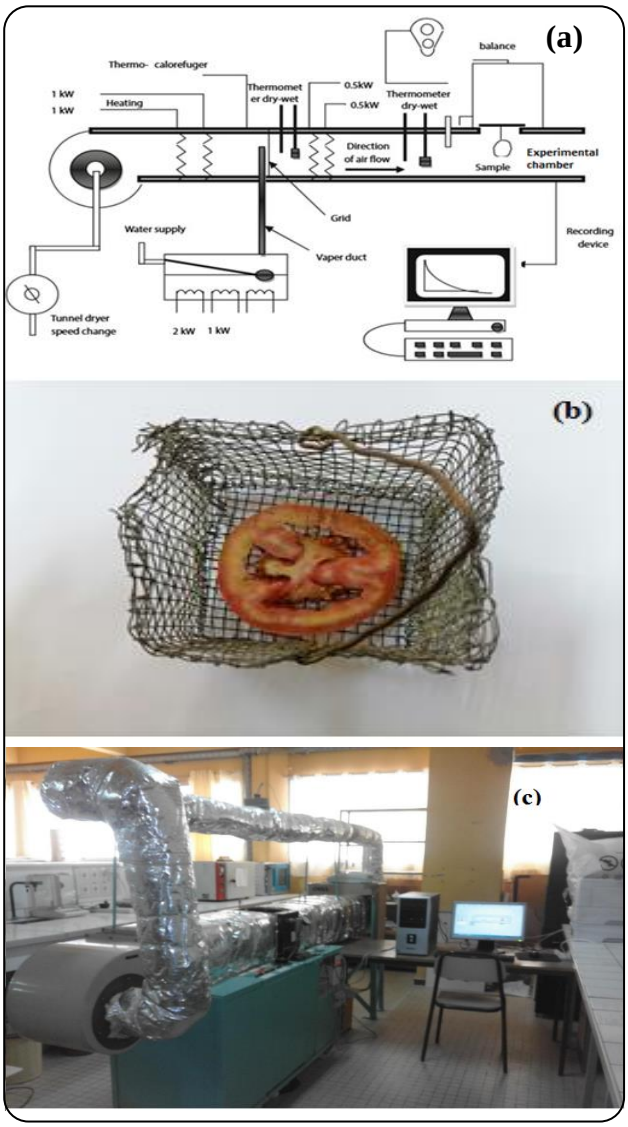

Fig.2: Hot air dryer pilot (a), a real figure of the tomato slices placed in the sample port (b) and the real experimental device (c)

were performed to reach the drying characteristic behaviours of several products studied in a temperature range from 20 to 100 °C; evaluating the drying profile and drying curves.

Tomatoes were cut in slices with 3 mm thickness, kept in sample holders with 50 g the weight of each sample. Tomatoes pieces were then organized with a thin layer form. The drying experiments were performed in a laboratory air tunnel (HILTON Air Conditioning Dryer), operating in closed cycle and equipped with a programmable controlling system for drying air parameters. The schematic of the dryer is given in Fig.2.

Initially, the system was run for at least half an hour to obtain the required air-drying temperature. Then, the samples holders were introduced in the experimental chamber. From this moment, we start following the variation in the weight of the product in terms of time. The mass of the product was continuously measured with a constant time interval (2 min) using an electronic scale and measurements were recorded by a computer. Then, dried tomato slices were put into an oven at 105 °C for 24 h to reach complete dehydration to establish the product water content at each moment:

$$X(t) = \frac{M(t)-Ms}{Ms} \quad (20)$$

where X the tomatoes' water content at every instant (t) of the drying process (kg of water / kg db);
M(t) is the tomatoes' mass at the time (t) and Ms the tomatoes dry mass.

Different thin layer models were used to describe the drying kinetics of agricultural products, as shown in Table 3. The regression was carried out using the Matlab R2013a computer program.

The adjustment between the experimentally established points and the model-predicted moisture content was judged by the correlation coefficient (R^2), the root means square error (RMSE) and the chi-square test (SSE). The model having a relatively high R^2 and relatively low SSE and RMSE suits best the drying process.

Effective moisture diffusivity

The effective moisture diffusivity shows the moisture movement rate of the food product during the drying process, covering all drying stages such as the first drying stage, a period of constant speed and another decreasing speed. The dependence of effective moisture diffusivity on Moisture Content (MR) is predicted by the Fick's second diffusion law, supposing the moisture movement at negligible shrinkage, constant temperature and diffusion coefficient. For an infinitely long slab drying, the equation can be expressed as follows [59,60]

$$\ln(MR) = \ln\left(\frac{8}{\Pi^2}\right) - \frac{\Pi^2.D_{eff}.t}{4.l^2} \quad (31)$$

where D_{eff} is the effective moisture diffusion coefficient (m^2/ s), t is the drying time (s) and l is the half-thickness of the slab (m).

The temperature dependence on the effective moisture diffusion coefficient (D_{eff}) is given by the Arrhenius equation, as illustrated in the Equation (32) [59,60]:

Table 3: Mathematical models used to fit drying kinetics

Model	Model equation		Reference
Midilli-Kucuk	$Xr = a.e^{(-c.t^d)}$+b.t	(21)	[51]
Two terms	$Xr = a.e^{(-c.t)} + b.e^{(-d.t)}$	(22)	[52]
Parabolic	$Xr = a + b.t + c.t^2$	(23)	[53]
Logarithmic	$Xr = a.e^{(-c.t)} + b$	(24)	[54]
DiffusionaApproach	$Xr = ae^{(-c.t)} + (1-a)e^{(-c.b.t)}$	(25)	[55]
Verma et al.	$Xr = ae^{(-c.t)} + (1-a)e^{(-b.t)}$	(26)	[56]
Wang and Singh	$Xr = 1 + a.t + b.t^2$	(27)	[57]
Henderson and Pabis	$Xr = ae^{(-b.t)}$	(28)	[58]
Newton	$Xr = e^{(-a.t)}$	(29)	[59]
Page	$Xr = e^{(-a.t^b)}$	(30)	[60]

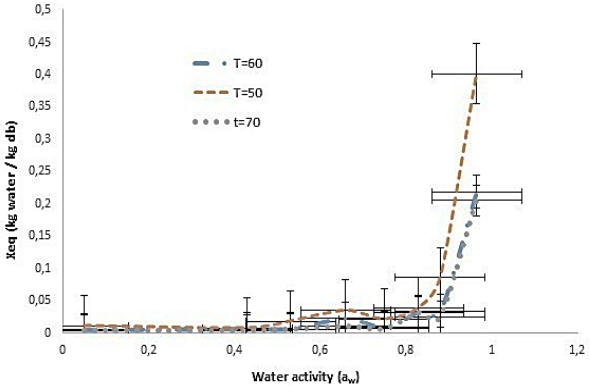

Fig. 3: Isotherm desorption of tomatoes at 50, 60 and 70°C

$$\ln\left(\frac{D_{eff}}{D_0}\right) = -\frac{Ea}{R.T} \quad (32)$$

Where D_0 the Arrhenius equation pre-exponential factor (m^2/s); Ea the activation energy for moisture diffusion (kJ/mol); R the universal gas constant (R = 0.008314 kJ/mol K) and T the absolute temperature (K).

RESULTS AND DISCUSSIONS

Desorption isotherm

The desorption curves of tomatoes are determined based on the static gravimetric method. We notice that the general aspect of the desorption isotherms of tomatoes, presented in Fig. 3, are of type III according to the BDDT classification.

We can observe the effect of temperature on the desorption isotherms in a water activity range from 0.053 to 0.958. The graphs show that, at a given water activity, the equilibrium moisture content in tomato is inversely proportion at temperature: an increase in temperature leads to the equilibrium water content reduction. On the other side, considering a fixed water content, the water activity increases with the temperature. Consequently, a reduction in the desorbed amount took place when temperature declined. Similar results have been observed by various researchers who have studied tomatoes desorption isotherm, such as *Viswanathan et al*.(2003) [63], and *Akanbi et al*. (2006) [64].

Table 4 shows the values of the constants and statistical parameters of all the chosen models to fit the isotherm curves at different tested temperatures.

The aim of this part is to determine the most adequate model to describe the desorption isotherms of our product. The regression was carried out using the MATLAB R2013a computer program. The models are compared based on statistical parameters such as the correlation coefficient (R^2) and RMSE. The best model will be the one with the highest R^2 and lowest value of RMSE.

These results (Table 4) demonstrate that the Guggenheim Anderson Boer (GAB) model is considered to be the most suitable for describing experimental desorption curves in the temperature range from 50 to 70 °C and a water activity ranging from 0.053 to 0.985, followed by the Adam, Oswin and Henderson models. It is clear that the GAB model had the highest value of R^2 correlation coefficient and the lowest value of RMSE. The GAB model has R^2 and RMSE values for sorption isotherms varying from 0.9932 to 0.9961 and 0.006615 to 0.01112, for temperatures ranging from 50 to 70 °C.

Giovanelli et al. (2002) [13] have measured and modeled the sorption isotherms of tomato compounds at 20 °C using the Guggenheim Anderson-de Boer (GAB) model. The movement of moisture into the dried tomato material and the molecular moisture transfer into its constituent

Table 4: Statistical model parameters and constants evaluated for fitting the experimental desorption isotherm curves

(a) Results which included numbers for A & B (Halsey to Oswin)						
(a)	T (°C)	A	B	SSE	R^2	RMSE
Halsey	50	0.011	0.778	0.0003	0.990	0.008
	60	0.018	0.761	0.0005	0.996	0.009
	70	0.012	0.713	0.0002	0.991	0.007
White and Eiring	50	249.300	-253.6	0.0002	0.993	0.006
	60	0.018	-142.2	0.0006	0.995	0.011
	70	319.600	-326.1	0.0002	0.994	0.006
Iglesias and Chirife	50	-0.004	0.008	0.0007	0.979	0.011
	60	-0.012	0.015	0.0018	0.986	0.017
	70	-0.007	0.008	0.0008	0.975	0.012
Caurie	50	-19.220	18.340	0.0009	0.975	0.012
	60	-18.140	17.850	0.0008	0.994	0.012
	70	-21.080	20.200	0.0006	0.979	0.011
Handerson	50	5.213	0.289	0.0006	0.984	0.010
	60	4.360	0.288	0.0006	0.995	0.010
	70	5.101	0.264	0.0004	0.987	0.008
Smith	50	-0.040	0.059	0.0103	0.717	0.041
	60	-0.079	0.110	0.0355	0.720	0.077
	70	-0.040	0.056	0.0098	0.702	0.040
Oswin	50	0.004	1.229	0.0003	0.989	0.008
	60	0.006	0.0005	1.2550	0.996	0.009
	70	0.002	1.344	0.0003	0.990	0.007

(b) Results which include numbers for A, B, C & D (Adam to GAB)								
(b)	T (°C)	A	B	C	D	SSE	R^2	RMSE
Adam	50	-0.039	0.993	-2.875	2.167	0.005	0.853	0.037
	60	-0.075	1.918	-5.597	4.217	0.013	0.894	0.058
	70	-0.039	0.962	-2.794	2.103	0.0048	0.854	0.348
Peleg	50	0.039	0.664	2.369	36.290	0.0002	0.993	0.008
	60	0.751	18.560	0.014	0.082	0.0001	0.991	0.005
	70	1.228	58.510	0.057	4.611	0.0002	0.993	0.008
Chung-Pfost	50	0.396	0.141	2.100	-0.115	0.0128	0.649	0.057
	60	0.948	0.123	3.148	-0.255	0.0528	0.584	0.103
	70	0.746	0.176	3.052	-0.134	0.0529	0.526	0.066
Langmuir	50	0.005	0.565	-1.014	---	0.0003	0.991	0.007
	60	0.021	0.415	-1.014	---	0.0006	0.995	0.011
	70	0.010	0.374	1.018	---	0.0002	0.993	0.007
GAB	50	1.427	1.016	0.152	---	0.0002	0.993	0.007
	60	1.356	1.014	0.184	---	0.0006	0.996	0.011
	70	1.268	1.023	0.305	---	0.0002	0.993	0.007

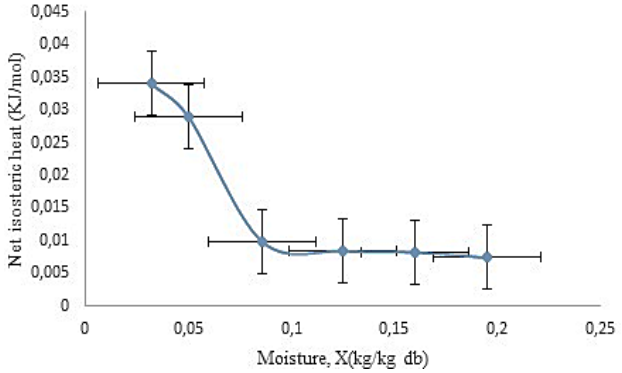

Fig.4: Isosteric heat of desorption

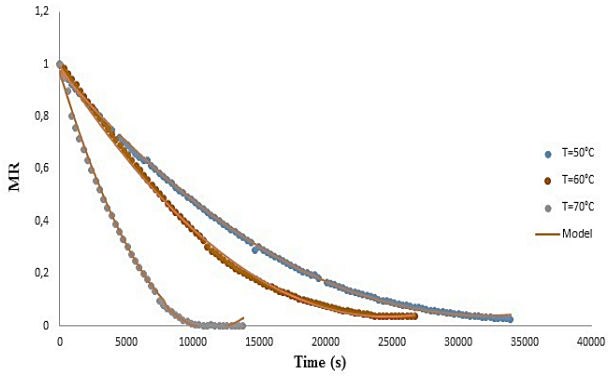

Fig.5: Experimental and model evolution of the reduced water content as a function of time

elements would produce a deviation of the idealized model condition. Water chemisorption resulted in the transformation of macromolecules [65]. The dehydrated tomato monomolecular moisture content was in the range from 0.152 to 0.305 kg/kg dry matter estimated from the GAB model. This is similar to the monolayer values previously reported for tomato by *Akanbi et al*.[64] and *Loumani et al*. [66]. Whereas *Dermanchi et al*. [67] and Chawla et al. [68] have found that the Leiva Díaz model and the modified Henderson's model are the most suitable models for the sorption isotherms of tomato pulp.

Isosteric heat

These results (Fig. 4) indicate that, with an increase in water content, the net isosteric heat decreases, implying that when the water content is low, the highest amount of energy is used to remove the emerging water in the product. *Tsami et al*.[69] have proposed that this is attributable to the existence of highly active polar sites enveloped with water molecules on the product surface, forming a monomolecular layer. *Iglesias* and *Chirifie* [70] have ascribed this phenomenon to the increase in the isosteric heat of sorption at low humidity caused by the greater resistance to the movement of water from the core of the sample to its surface. The sorption isosteric heats are elevated at low moisture contents (< 20%) and the subsequent isosteric heats of TS desorption decreases sharply with the increase in the product moisture content.

CONVECTIVE DRYING

Influence of air temperature on the drying kinetics

The initial water content of tomato tranches was 93.2 ± 0.5 (g water / g dry sample) and reduced to 4.372, 0.921 and 0.513 g water/g dry product for tomato slices processed at 50, 60 and 70 °C of the hot air dryer, respectively, at fixed air velocity of 1.4 m/s and relative humidity (RH) equal to 30 %.

The drying curves of tomato slices by the hot air dryer are reported in Fig.5.

There were similar drying profiles for tomatoes [71], tomato slices [72], tomato seeds [73] and tomato paste [74]. According to Fig.5, the drying time strongly depends on the temperature. Indeed, when the temperature increases; the drying time decreases, this dependence is clear for example at time t = 6000 s, where the value of the reduced water content is equal to 0.7187, 0.6345 and 0.5187 kg water/kg db for temperatures of 50, 60 and 70 °C, respectively, and at a fixed air velocity equal to 1.4 m/s. As expected, the highest temperature needed less time to dry TS that required at the lowest temperature. The decreasing of the moisture content with increase in the time period at all the studied temperatures shows that drying of the tomato slices occurred in the falling rate period. The drying air temperature affected on the reduced water content and the drying time is explained by the product heat increase with the air temperature. This increase leads to an expansion of the bonds of the water molecules, which promotes the evaporation of the contained water. The increase in temperature leads to a difference in partial pressure of the water vapor between the surface of the product and the drying air. The increase in drying potential and the reduction in drying time is explained by the fact that the increase in temperature leads to an increase in the intensity of heat transfer. The increase in drying temperature is responsible for the increase in the energy of the water molecules, thus accelerating the migration of water inside the product, which can escape more easily and rapidly.

Table 5: The different results of the kinetic models

Model	T(C°)	a	b	c	d	SSE	R^2	RMSE
Midilli-Kucuk	50	0.96	-0.003	0.21	1.20	0.0096	0.999	0.009
	60	0.99	-0.009	0.72	1.30	0.0140	0.996	0.018
	70	0.95	-0.008	0.64	1.39	0.0144	0.996	0.019
Two terms	50	49.63	-48.61	0.41	0.42	0.0516	0.994	0.022
	60	37.73	-36.61	1.16	1.17	0.0631	0.985	0.038
	70	24.17	-23.12	0.47	0.45	0.0320	0.992	0.029
Parabolic	50	0.97	-0.21	0.012	---	0.006	0.999	0.008
	60	1.02	-0.61	0.092	---	0.007	0.998	0.013
	70	1.00	-0.60	0.092	---	0.010	0.997	0.015
Logarithmic	50	1.13	-0.12	0.235	---	0.018	0.998	0.012
	60	1.20	-0.100	0.749	---	0.022	0.995	0.022
	70	1.20	-0.17	0.610	---	0.029	0.992	0.027
Diffusional approach	50	-0.66	0.99	0.210	---	0.118	0.987	0.033
	60	8.30	0.91	0.414	---	0.037	0.991	0.029
	70	14.69	0.94	0.369	---	0.028	0.993	0.027
Verma et al.	50	4.88	-0.14	0.164	---	0.014	0.998	0.011
	60	9.17	-0.37	0.405	---	0.037	0.991	0.029
	70	6.73	-0.33	0.385	---	0.028	0.993	0.027
Wang and Singh	50	-0.22	0.013	---	---	0.017	0.998	0.012
	60	-0.60	0.09	---	---	0.009	0.997	0.014
	70	0.60	0.09	---	---	0.010	0.997	0.016
Henderson and Pabis	50	1.05	0.31	0.094	---	0.093	0.989	0.029
	60	1.15	0.97	0.074	---	0.074	0.982	0.041
	70	1.08	0.88	0.095	---	0.094	0.976	0.048
Newton	50	0.30	---	---	---	0.118	0.987	0.032
	60	0.85	---	---	---	0.118	0.987	0.032
	70	0.82	---	---	---	0.122	0.969	0.054
Page	50	0.230	1.19	---	---	0.029	0.997	0.016
	60	0.74	1.37	---	---	0.023	0.994	0.023
	70	0.72	1.34	---	---	0.025	0.994	0.025

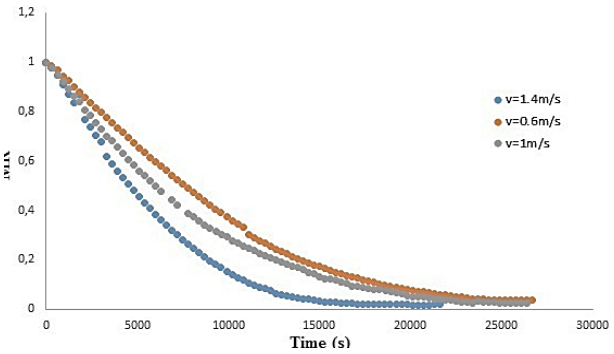

Fig. 6: Experimental reduced water content evolution as function of time and air velocity

The estimated drying rate constants, the dimensionless constants and other parameters for every drying model are shown in Table 5 for each drying temperature. The R^2 and RMSE values for each model and the drying temperature reveal the best-fit model. Indeed, the highest R^2 values and lowest RMSE relate to the model that best fits the drying kinetics of the tomato slices.

Table 6: Evolution of drying time with hot air velocity

Air velocity (m/s)	Drying time (h)
0,6	5.76
1	5.41
1,4	4.89

For the studied hot air dryer, the logarithmic model (at drying temperatures of 50 to 70 °C) was found to be the best-fitted model with R^2 values of 0.9992, 0.9982 and 0.9975, and RMSE values of 0.0079, 0.013 and 0.015 for the temperatures 50, 60 and 70 °C, respectively.

Influence of air velocity on drying kinetics

Fig.6 exhibits the product drying times presented in Table 6 to reach the equilibrium for the three speed values studied: 0.6 m/s, 1 m/s and 1.4 m/s for a fixed temperature of 60 °C and relative humidity of 30 %.

Table 7: Diffusion parameters and Arrhenius equation of tomato slices for hot air drying at different temperatures and at fixed drying air velocity = 1.4 m/s

Temperature(°C)	D_{eff}*(10^{-7}) (m^2/s)	Ln(D_0)(m^2/s)	Ea (kJ/mol)	R^2
50	2.028	16.378	42.140	0.9959
60	3.042			
70	5.071			

Table 8: A comparative study with previous studies

Drying technique	**Drying time**		**References**
Microwave drying	10h		[80]
hot air drying	10h		[81]
hot air drying	10.2h		[82]
solar dryer	12.5h		[83]
Osmotic and convective drying Process	3.5 – 6.5 h		[84]
hot air drying	4.89h		This work
Drying technique	**Deff**	**Ea**	**References**
Hot air drying	0.98 10^{-10}- 6.38 10^{-10}	12.23-25.76	[85]
Osmotic and convective drying Process	0.78 10^{-10}- 1.30 10^{-10}	29.67	[84]
Hot air drying	3.37 10^{-10}- 58.2 10^{-10}	196- 198	[86]

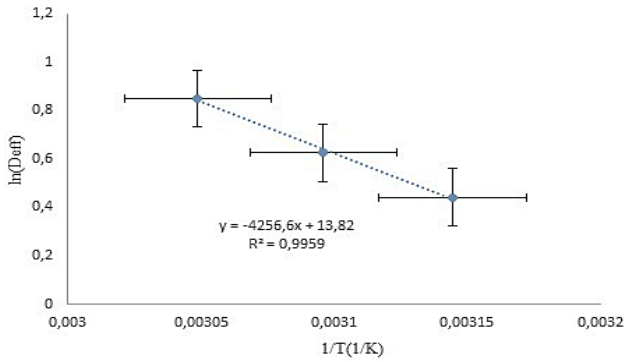

Fig. 7: Arrhenius relationship between effective moisture diffusion (D_{eff}) of tomato slices and temperature for hot air drying and at fixed drying air velocity = 1.4 m/s

The obtained results are in excellent accord with the literature [75]. Indeed, the moisture content decreased as the velocity of the drying air increased. The drying velocity, however, increases when the drying air velocity increases. *Daguenet* [75] has explained this phenomenon by describing the drying rate in terms of the water vapor transfer coefficient. This factor has an important effect on the drying rate by promoting a good mass and heat transfer manifested as a very fast drying speed.

Effective moisture diffusivity

Table 7 presents tomato effective moisture diffusivity and activation energy at different drying parameters. The effective moisture diffusivity (D_{eff}) during the tomato drying process ranged between 52.028 10^{-7}m/sand 5.071 10^{-7}m/s.

This is in the range of biological materials [76]. Diffusivity was found to rise with increasing temperatures because of higher moisture migration [77].

The tomato effective moisture diffusivity (D_{eff}) greatly increased with increasing temperature and was found to be proliferate at higher temperature. The calculated values of Deff for tomatoes drying were 2.028 10^{-7}, 3.042 10^{-7} and 5.071 10^{-7} m^2/s at 50, 60 and 70 °C, respectively. The activation energy was calculated using Equation (7). The diffusion activation energy for the drying tomato slices appears to be valid and reasonable (Table7 and Fig.7) when compared with the results of D_{eff} and Ea found by *Hosainpour et al*. for the ohmicpre drying of tomato paste [78] and *Demiray et al*. for tomato slices [79]. The figure shows a linear relationship duo to the Arrhenius-type dependence (R^2=0.9959). From the slope of this line, an activation energy value of 42.140 kJ/mol was determined for tomatoes drying

Table 8 shows a comparative study with previous works studying the tomato drying by different techniques.

Solar design consideration

The solar dryer was designed based on the producer described by [87]. The following data were considered in the design of the solar dryer system: (i) The amount of moisture to be removed from a given quantity of wet tomato, (ii) Harvesting period during which the drying is needed, (iii) The daily sunshine hours for the selection of the total drying time, (iv) The quantity of air needed

Table 9: Design conditions and assumptions

Item	Condition/Assumption
Drying period	July-August
Loading rate	100 kg sliced tomato
Initial content	0.93 kg/kg
Final content	0.05 kg/kg
Ambient temperature	40 °C
Ambient relative humidity	30 %
Maximum allowable temperature	75 °C
Drying time per day	10 h
Efficiency	45%
Wind speed	2 m/s
Thickness of sliced	4 mm
Solar irradiation	1711,038 kWh/m²
Declination	30°
Orientation	180 °

Table 10: Design parameters

Item	Condition/Assumption
Initial humidity	July-August
Mass of water evaporated	80 %
Volumetric flow rate	340 m^3/h
Area	9 m^2
Nominal heating power	75 kW
hot water coverage rate	61 %
Total surface irradiation	16624 kWh
Drying rate	3.75 kg/h
Water evaporated	75 kg

for drying, (v) Daily solar radiation to determine energy received by the dryer per day, (vi) Wind speed.

The size of the dryer was determined as a function of the drying area needed per kilogram of product. The drying temperature was established as a function of the maximum limit of temperature the product might support.

The conditions and assumptions used for the design of tomato dryer were summarized in Table 9. From the conditions, assumptions and correlations, the values of the design parameters were calculated, and the results are grouped in Table 10.

The optimal drying temperature was 70 ˚C and final moisture content of tomato for storage is 5 % wet basis. The corresponding relative humidity is 85 %. Many conditions and assumptions applicable to the region are used to design and sizing the installation of drying. The loading rate is 100 kg of sliced tomato. From the thermodynamic and kinetics of drying tomato the amount of energy required for the drying process is calculated, and consequently the solar energy also.

The preliminary economic study, following the calculation, proves to bring positive results and tends towards the construction of the drying plant.

CONCLUSIONS

The desorption isotherms were determined by the gravimetric method and then the fitting showed that the GAB model is the most appropriate for the desorption of tomato slices, with both the highest coefficient values (R^2) and the lowest basic standard error values at a temperature ranging from50 and 70 °C. The net desorption isosteric heats were determined by combining the GAB model with the Clausius-Clapeyron equation. The heat of desorption was found to be inversely proportional to the amount of moisture.

The convective drying kinetics of tomato slices were studied at various temperatures and drying air velocities. The obtained results demonstrated that the product drying kinetics have a single drying phase, the decreasing rate drying phase. The TS drying kinetic experimental data were adjusted by various mathematical models. The parabolic model was found to be the most appropriate to describe the drying kinetics experimental data in for a temperature ranging from 50 to 70 °C, velocity of 0.5 to 1.44 m/s and relative humidity of 30%. The selected model performance in describing the drying kinetics at different operating conditions was established. The drying under different operating conditions was confirmed by the statistical analysis of the experimental data (highest correlation coefficient and lowest root mean square error). The effective moisture diffusivity and the activation energy were tested by the second Fick's law. The values of effective moisture diffusivity were ranged from 2.028 10^{-7} to 5.071 10^{-7} m^2/s. The activation energy was calculated to be 42.140 kJ/mol. The experimental results obtained

during this study show that it is possible to design a solar tomato drying plant.

Finally, from these preliminary experimental results, we believe that a solar drying will help poor farmers to obtain a sustainable income due to the very high selling prices of dried products, and allows the government to circumvent the problems of rising energy prices in recent years. The next step will be focused on constructing the solar dryer in order to conduct actual data in the field.

Nomenclature

Abbreviation	Signification
aw	Water activity, %
M_h	Mass of the samples before drying, kg
M_s	Mass of the samples after drying, kg
X_{eq}	Water content of the samples at equilibrium, kg/kg
Δhd	Heat of sorption, J/mol
ΔHvap	Heat of water vaporization, J/mol
ΔHd	Isosteric heat of sorption, J/mol
T	Temperature, K
V	Air velocity, m/s
RH	Relative humidity, %
R^2	Correlation coefficient
RMSE	Root mean square error
SSE	Chi-square test
X	Tomatoes' water content at every instant (t) of the drying process, kg/kg
M(t)	Tomatoes' mass at the time (t), K
Ms	Tomatoes dry mass, kg
MR	Moisture content, kg/kg
D_{eff}	Effective moisture diffusion coefficient, m^2/s
t	Drying time, s
l	Half-thickness of the slab, m
D_0	Arrhenius equation pre-exponential factor, m^2/s
Ea	Activation energy for moisture diffusion, J/mol
R	Universal gas constant, J/(mol.K)
v	Air velocity, m/s
GAB	Guggenheim Anderson Boer model
A,B,C and D	Statistical isotherm model constants
A, b, c and d	Statistical kinetic model constants
X_{jcal}	Calculated values of the water content at equilibrium, kg/kg
X_{exp}	Experimental values of the water content at equilibrium, kg/kg
n_p	Model constants number
N	Experimental points number
X_m	The value of the arithmetic means of the experimental values of the water content at equilibriu, kg/kg

Received : Oct. 14, 2022 ; Accepted : Dec. 26, 2022

REFERENCES

[1] Perveen R., Suleria H.A.R., Anjum F.M., Butt M.S., Pasha I., Ahmad S., Tomato (Solanum Lycopersicum) Carotenoids and Lycopenes Chemistry; Metabolism, Absorption, Nutrition, and Allied Health Claims-A Comprehensive Review, *Crit. Rev. Food Sci. Nutr.*, **55 (7)**: 919–929 (2015).

[2] Rubén D., Gullon P., Pateiro M., Munekata P.E.S., Zhang W., Lorenzo J.M., Tomato as Potential Source of Natural Additives for Meat Industry, *Antioxidants*, **9(1)**: 73 (2020).

[3] Ochida C.O., Itodo A.U., Nwanganga P.A., A Review on Postharvest Storage, Processing and Preservation of Tomatoes (Lycopersicon Esculentum Mill), *Asian Food Sci. J.*, **6(2)**: 1–10 (2018).

[4] Cheng H.M., Koutsidis G., Lodge J.K., Ashor A.W., Siervo M., Lara J., Lycopene and Tomato and Risk of Cardiovascular Diseases: A Systematic Review and Meta-Analysis of Epidemiological Evidence, *Crit. Rev. Food Sci. Nutr.*, **59(1)**: 141–158 (2019).

[5] Badaoui O., Hanini S., Djebli A., Haddad B., Benhamou A., Experimental and Modelling Study of Tomato Pomace Waste Drying in a New Solar Greenhouse: Evaluation of New Drying Models, *Renew. Energy*, **133**: 144–155 (2019).

[6] Burg P. Fraile P., Vitamin C Destruction During the Cooking of a Potato Dish, *LWT - Food Sci. Technol.*, **28(50)**: 506–514 (1995).

[7] Sonawane A., Chauhan O.P., Semwal S.D., Semwal A.D., Drying Characteristics and Lycopene Degradation Kinetics of Tomato Soup, *Chem. Data Collect.*, **35**: 100757 (2021).

[8] Djebli A., Hanini S., Badaoui O., Boumahdi M., A New Approach to the Thermodynamics Study of Drying Tomatoes in Mixed Solar Dryer, *Sol. Energy*, **193**:164–174 (2019).

[9] Dufera L.T., Hofacker W., Esper A., Hensel O., Physicochemical Quality of Twin Layer Solar Tunnel Dried Tomato Slices, *Heliyon*, **7(5)**: e07127 (2021).

[10] Azeez L., Adebisi S.A., Oyedeji A.O., Adetoro R.O, Tijani K.O, Bioactive Compounds' Contents, Drying Kinetics and Mathematical Modelling of Tomato Slices Influenced by Drying Temperatures and Time, *J. Saudi Soc. Agric. Sci.*, **18(2)**: 120–126 (2019).

[11] Miccio M., Pierri R., Cuccurullo G., Metallo A., Brachi P., Process Intensification of Tomato Residues Drying By Microwave Heating: Experiments and Simulation, *Chem. Eng. Process. - Process Intensif.*, **156**: 108082 (2020).

[12] Gaware T.J., Sutar N., Thorat B.N., Drying of Tomato Using Different Methods: Comparison of Dehydration and Rehydration Kinetics, *Dry. Technol.*, **28(5)**: 651–658 (2010).

[13] Giovanelli G., Zanoni B., Lavelli V., Nani. R., Water Sorption, Drying and Antioxidant Properties of Dried Tomato products, *J. Food Eng.*, **52(2)**: 135–141 (2002).

[14] Abbasi H., Layeghiniya N., Mohammadi S., Karimi S., Effect of Fruit Thickness on Microwave Drying Characteristics of *Myrtus Communis* L., *Iran. J. Chem. Chem. Eng. (IJCCE)*, **41(1)**: 222-236 (2022).

[15] Khodaparast Haghi A., Ghanadzadeh H., Rondot D., Experimental Survey on Microwave Drying of Porous Media, *Iran. J. Chem. Chem. Eng.(IJCCE)*, **24(2)**: 1–10 (2005).

[16] Honarvar B., Mowla D., Safekordi A.A., Experimental and Theoretical Investigation of Drying of Green Peas in a Fluidized Bed Dryer of Inert Particles Assisted by Infrared Heat sSource, *Iran. J. Chem. Chem. Eng. (IJCCE)*, **32(1)**: 83–94 (2013).

[17] Dehbozorgi F., Khorshidi Malahmadi J., Niyazi S., Improving Three Phase Modeling of Fluidized Bed Dryer, *Iran. J. Chem. Chem. Eng.*, **33(2)**: 99–105 (2014).

[18] Taghinezhad E., Rasooli Sharabiani V., Kaveh M., Modeling and Optimization of Hybrid HIR Drying Variables for Processing of Parboiled Paddy Using Response Surface Methodology, *Iran. J. Chem. Chem. Eng. (IJCCE)*, **38(4)**: 251–260 (2019).

[19] Pang S. Mujumdar A.S., Drying of Woody Biomass for Bioenergy: Drying Technologies and Optimization for an Integrated Bioenergy Plant, *Dry. Technol.*, **28(5)**: 690–701 (2010).

[20] Mujumdar A.S., Current Status and Future Trends, *Ind. Dry. Technol.*, **200**1: 112–113 (2001).

[21] Seyedabadi E., Khojastehpour M., Abbaspour-Fard M.H, Convective Drying Simulation of Banana Slabs Considering Non-Isotropic Shrinkage Using FEM with the Arbitrary Lagrangian–Eulerian Method, *Int. J. Food Prop.*, **20(1)**: S36–S49 (2017).

[22] Kaveh M., Jahanbakhshi A., Abbaspour-Gilandeh Y., Taghinezhad E., Moghimi. M.B.F, The Effect of Ultrasound Pre-Treatment on Quality, Drying, and Thermodynamic Attributes of Almond Kernel under Convective Dryer using ANNs and ANFIS Network, *J. Food Process Eng.*, **41(7)**: 1–14 (2018).

[23] Süfer Ö., Sezer S., Demir H., Thin Layer Mathematical Modeling of Convective, Vacuum and Microwave Drying of Intact and Brined Onion Slices, *J. Food Process. Preserv.*, **41(6)**: (2017).

[24] Torki Harchegan M., Sadeghi M., Ghanbarian D., Moheb A., Dehydration Characteristics of Whole Lemons in a Convective Hot Air Dryer, *Iran. J. Chem. Chem. Eng. (IJCCE)*, **35(3)**: 65–73 (2016).

[25] Azzouz S., Hermassi I., Chouikh R., Guizani A., Belghith A., The Convective Drying of Grape Seeds: Effect of Shrinkage on Heat and Mass Transfer, *J. Food Process Eng.*, **41(1)**: 1–8 (2018).

[26] Sajawal M., Rehman T.U., Ali H.M., Sajjad U., Raza A., Bhatti M.S., Experimental Thermal Performance Analysis of Finned Tube-Phase Change Material Based Double Pass Solar Air Heater, *Case Stud. Therm. Eng.*, **15**: 100543 (2019).

[27] Aboghrara A.M., Baharudin B.T.H.T., Alghoul M.A., Adam N.M., Hairuddi A.A., Hasan H.A, Performance Analysis of Solar Air Heater with Jet Impingement on Corrugated Absorber Plate, *Case Stud. Therm. Eng.*, **10**: 111–120 (2017).

[28] Mzad H., Bey K., Khelif R., Investigative Study of the Thermal Performance of a Trial Solar Air Heater, *Case Stud. Therm. Eng.*, **13**: 100373 (2019).

[29] Abu-Hamdeh N.H., Bantan R.A.R., Khoshvaght-Aliabadi M., Alimoradi A., Effects of Ribs on Thermal Performance of Curved Absorber Tube Used in Cylindrical Solar Collectors, *Renew. Energy*, **161**: 1260–1275 (2020).

[30] Bella F., Boosting the Efficiency of Aqueous Solar Cells: A Photoelectrochemical Estimation on the Effectiveness of $TiCl_4$ Treatment, *Electrochim. Acta.*, **302**: 31–37 (2019).

[31] Galliano S., Finely Tuning Electrolytes and Photoanodes in Aqueous Solar Cells by Experimental Design, *Sol. Energy*, **163**: 251–255 (2018).

[32] Vijayan S., Arjunan T.V., Kumar. A., Fundamental Concepts of Drying, *Sol. Dry. Technol. Green Energy Technol.*, **0(9789811038327)**: 3–38 (2017).
[33] Schiraldi A., Fessas D., Signorelli M., Water Activity In Biological Systems - A Review, *Polish J. Food Nutr. Sci.*, **62(1)**: 5–13 (2012).
[34] Bourdoux S., Li D., Rajkovic A., Devlieghere F., Uyttendaele M., Performance of Drying Technologies to Ensure Microbial Safety of Dried Fruits and Vegetables, *Compr. Rev. Food Sci. Food Saf.*, **15(6)**: 1056–1066 (2016).
[35] Jannot Y., Isothermes de Sorption : Modeles et Determination Activite de l ' eau Formes et Modèles des Isothermes de Sorption, 1–16 (2008).
[36] Hssaini L., Hygroscopic Proprieties of Fig (Ficus Carica L.): Mathematical Modelling of Moisture Sorption Isotherms and Isosteric Heat Kinetics, *South African J. Bot.*, 1–10 (2020).
[37] Smith S.E, The Sorption of Water Vapor by High Polymers, *J. Am. Chem. Soc.*, 69(3) 646–651 (1947).
[38] Iglesias J., Chirife H.A, An Equation for fitting Uncommon Water Sorption Isotherms in Foods., *Leb. und -Technologie*, **14**: 111–117 (1981).
[39] Castillo M.D., Martnez E.J., Gonzlez H.H.L., Pacin A.M., Resnik S.L., Study of Mathematical Models Applied to Sorption Isotherms of Argentinean Black Bean Varieties, *J. Food Eng.*, **60(4)**: 343–348 (2003).
[40] Peleg M., Assessment of a Semi-Empirical Four Parameter General Model for Sigmoid Moisture Sorption Isotherms, *J. Food Process Eng.*, **16(1):** 21–37 (1993).
[41] Van Der Berg S., Bruin C., Water Activity and its Estimation in Food Systems; Theoretical Aspects. In Water Activity: Influences on Food Quality, Acad. Press. New York., 1–61 (1981).
[42] Oswin C.R., The Kinetics of Package Life. III. The Isotherm, *J. Soc. Chem. Ind.*, **65(12)**: 419–421 (1946).
[43] Chirife H.A., Iglesias J., Equations for fitting Water Sorption Isotherms of Foods: Part I. A Review, *J. Food Technol.*, **13**: 159–174 (1978).
[44] Halsey G., Physical Adsorption on NonUniform Surfaces, **931**: (1948).
[45] Langmuir I., The Constitution and Fundamental Properties of Solids and Liquids. Part i. Solids, *J. Am. Chem. Soc.*, **46**: 1361–1362 (1916).
[46] Henderson S., A Basic Concept of Equilibrium Moisture, *Agric. Eng.*, **33**: 29–32 (1952).
[47] Chung D., Pfost H., Adsorption and Desorption of Water Vapour by Cereal Grains and Their Products, *Trans. ASEA*, **10**: 549–551 (1967).
[48] Jmai S., Bagane M., Kint T.M.Q., Di-calcium phosphate; Thermodynamics and Kinetics Study, *Int. J. Sci. Eng. Res.*, **9(5)**: 389–402 (2018).
[49] Abdenouri N., Idlimam A., Kouhila M., Sorption Isotherms and Thermodynamic Properties of Powdered Milk, *Chem. Eng. Commun.*, **197(8)**: 1109–1125 (2010).
[50] Tsami E., Maroulis Z.B., Marinos-Kouris D., Saravacos G.D., Heat of sorption of water in dried fruits *Int. J. Food Sci. Technol.*, **25(3)**: 350–359 (1990).
[51] Midilli A., Kucuk H., Yapar Z., A New Model for Single-Layer Drying, *Dry. Technol.*, **20**: 1503–1513 (2002).
[52] Henderson S., Progress in Developing the Thin Layer Drying Equation, *Trans. Am. Soc. Agric. Eng.*, **17**: 1167–1168 (1974).
[53] Darvishi H., Azadbakht M., Rezaeiasl A., Farhang A., Drying Characteristics of Sardine Fish Dried with Microwave Heating, *J. Saudi Soc. Agric. Sci.*, **12(2)**: 121–127 (2013).
[54] Chandra P.K. Singh R.P, Applied Numerical Methods for Food and Agricultural Engineers, *CRC Press. Boca Rat.*, **512**: (1994).
[55] Yaldiz O., Ertekin C., Uzun H., Mathematical Modeling of Thin Layer Solar Drying of Sultana Grapes, *Energy*, **26**: 457–465 (2001).
[56] Verma L., Bucklin R., Endan J., Wratten F., Effects of Drying Air Parameters on Rice Drying Models, *Trans. Am. Soc. Agric. Eng.*, **28**: 296–301, (1985).
[57] Wang C., Singh R., A Single Layer Drying Equation for Rough Rice, *Trans. Am. Soc. Agric. Eng.*, 1–17 (1978).
[58] Henderson M., Pabis S., Grain Drying Theory: IV the Effect of Airflow Rate on Drying Index, *J. Agric. Eng. Res.*, **7**: 85–89 (1962).
[59] Lewis W., The Rate of Drying of Solid Materials, *Ind. Eng. Chem.*, **13**: 427–432 (1921).
[60] Page G., Factors Influencing the Maximum Rate of Air Drying Shelled Corn in Thin-Layers, *Purdue Univ. West Lafayette, Indiana* (1949).

[61] Golmohammadi M., Foroughi-Dahr M., Rajabi-Hamaneh M., Shojamoradi A.R., Hashemi S.J., Study on Drying Kinetics of Paddy Rice: Intermittent Drying, *Iran. J. Chem. Chem. Eng. (IJCCE)*, **35(3)**: 105–117 (2016).

[62] Chen D., Zheng Y., Zhu X., Determination of Effective Moisture Diffusivity and Drying Kinetics for Poplar Sawdust by Thermogravimetric Analysis under Isothermal Condition, *Bioresour. Technol.*, **107**: 451–455 (2012).

[63] Viswanathan R., Jayas D.S., Hulasare R.B, Sorption Isotherms of Tomato Slices and Onion Shreds, *Biosyst. Eng.*, **86(4)**: 465–472 (2003).

[64] Akanbi C.T., Adeyemi R.S., Ojo. A., Drying Characteristics and Sorption Isotherm of Tomato Slices, *J. Food Eng.*, **73(2)**: 157–163 (2006).

[65] Wang N., Brennan J.G., Moisture Sorption Isotherm Characteristics of Potatoes at four Temperatures, *J. Food Eng.*, **14(4)**: 269–287 (1991).

[66] Loumani *et al.*, Experimental Measurement of Isothermal Sorption, Microbiological and Physicochemical Analysis of Dried Tomatoes Cultivated in Adrar, Algeria, *Int. J. Des. Nat. Ecodynamics*, **15(5)**: 721–728 (2020).

[67] Demarchi S.M., Quintero Ruiz N.A., De Michelis A., Giner S.A., Sorption Characteristics of Rosehip, Apple and Tomato Pulp Formulations as Determined by Gravimetric and Hygrometric Methods, *LWT - Food Sci. Technol.*, **52(1)**: 21–26 (2013).

[68] Chawla C., Kaur D., Oberoi D.P.S., Sogi D.S., Drying Characteristics, Sorption isotherms, and Lycopene Retention of Tomato Pulp, *Dry. Technol.*, **26(10)**: 1257–1264 (2008).

[69] Tsami E., Net isosteric Heat of Sorption in Dried Fruits, *J. Food Eng.*, **14 (4)**: 327–335 (1991).

[70] Iglesias J., Chirife H.A., Isosteric Heats of Water Vapor Sorption on Dehydrated Foods. Part II: Hysteresis and Heat of Sorption Comparison with BET Theory, *LWT Leb. Wissensch Technol.*, 123-127 (1976).

[71] Doymaz I., Air-Drying Characteristics of Tomatoes, *J. Food Eng.*, **78(4)**: 1291–1297 (2007).

[72] Rajkumar P., Kulanthaisami S., Raghavan G.S.V., Gariépy Y., Orsat V., Drying Kinetics of Tomato Slices in Vacuum Assisted Solar and Open Sun Drying Methods, *Dry. Technol.*, **25(7–8)**: 1349–1357 (2007).

[73] Sogi D.S., Shivhare U.S., Garg S.K, Bawa A.S., Water Sorption Isotherm and Drying Characteristics of Tomato Seeds, *Biosyst. Eng.*, **84(3)**: 297–301 (2003).

[74] Brygidyr A.M., Rzepecka M.A., McConnell M.B., Characterization and Drying of Tomato Paste Foam by Hot Air and Microwave Energy, *Can. Inst. Food Sci. Technol. J.*, **10(4)**: 313–319 (1977).

[75] Michel Daguenet, Les Séchoirs Solaires: Théorie et Pratique, (1985).

[76] Nourhène B., Mohammed K., Nabil K., Experimental and Mathematical Investigations of Convective Solar Drying of Four Varieties of Olive Leaves, *Food Bioprod. Process.*, **86(3)**: 176–184 (2008).

[77] Meziane S., Drying Kinetics of Olive Pomace in a Fluidized Bed Dryer, *Energy Convers. Manag.*, **52(3)**: 1644–1649, (2011).

[78] Hosainpour A., Darvishi H., Nargesi F., Fadavi A., Ohmic Pre-Drying of Tomato Paste, *Food Sci. Technol. Int.*, **20(3)**: 193–204 (2014).

[79] Demiray E., Tulek Y., Yilmaz Y., Degradation Kinetics of Lycopene, β-Carotene and Ascorbic Acid in Tomatoes During Hot Air Drying, *LWT - Food Sci. Technol.*, **50(1)**: 172–176, (2013).

[80] Al-Harahsheh M., Al-Muhtaseb A.H., Magee T.R.A., Microwave Drying Kinetics of Tomato Pomace: Effect of Osmotic Dehydration, *Chem. Eng. Process. Process Intensif.*, **48(1)**: 524–531 (2009).

[81] Demiray E., Tulek Y., Yilmaz Y., Degradation Kinetics of Lycopene, β-Carotene and Ascorbic Acid in Tomatoes During Hot Air Drying, *LWT*, **50(1)**: 172–176 (2013).

[82] Marfil P.H.M., Santos E.M., Telis V.R.N., Ascorbic Acid Degradation Kinetics in Tomatoes at Different Drying Conditions, *Lwt*, **41(9)**: 1642–1647 (2008)

[83] Erick César L.V., Ana Lilia C.M., Octavio G.V., Isaac P.F., Rogelio B.O., Thermal Performance of a Passive, Mixed-Type Solar Dryer for Tomato Slices (Solanum Lycopersicum), *Renew. Energy*, **147**: 845–855 (2020).

[84] Revaskar V.A., Pisalkar P.S., Pathare P.B., Sharma G.P., Dehydration Kinetics of Onion Slices in Osmotic and Air Convective Drying Process, *Res. Agric. Eng.*, **60(3)**: 92–99 (2014).

[85] Madamba P., Driscoll R., Buckle K., The Thin-Layer Drying Characteristics of Garlic Slices, *J. Food Eng.*, **29**: 75–97 (1996).

[86] Afolabi T.J., Tunde-Akintunde T.Y., Oyelade O.J., Influence of Drying Conditions on the Effective Moisture Diffusivity and Energy Requirements of Ginger Slices, *J. Food Res.*, **3(5)**: 103 (2014).

[87] Al-Busoul M., Design of Fruits Solar Energy Dryer under Climatic Condition in Jordan, *J. Power Energy Eng.*, **05(02)**:123–137 (2017).